

Institute of Meteorology, University of Natural Resources and Applied Life Sciences Vienna (BOKU),
Vienna, Austria

Synoptic and regional patterns of heavy precipitation in Austria

Petra Seibert, Andreas Frank, and Herbert Formayer

With 4 Figures

Submitted to
THEORETICAL AND APPLIED CLIMATOLOGY

Revised Version, 14th July 2005

Summary

Seven synoptic patterns responsible for heavy precipitation in Austria were identified with a trajectory clustering method. Back trajectories at different levels, at different times during each day, and from different locations in Austria were utilised together with one potential vorticity value. In addition, seven regions within Austria with similar daily precipitation were identified. The response of heavy precipitation in each of these regions to the synoptic patterns was studied. The results correspond to the synoptic experience and reflect known meteorological situations, such as southerly and northerly Stau or the Vb pattern. The analyses are based on the 15-year re-analysis of the ECMWF (1979–1993), used to calculate the back trajectories, and daily precipitation sums of 131 climate stations in Austria. This paves the way to future applications in climate change research, as the necessary input data are also available from global climate models. The clustering was performed with a promising new procedure, a combination of hierarchical and iterative (K-means) clustering.

1 Introduction

Catastrophes caused by heavy precipitation are not uncommon in Austria. In August 2002, two such events within ten days caused severe and widespread damage in Austria, in the Czech Republic and in Germany (Becker and Grünewald, 2003; Kubát et al., 2003). In Austria, this triggered to a short research programme called Startclim (Kromp-Kolb and Schwarzl, 2003) which was conducted in 2003. Its thematic approach was rather broad, including natural science, engineering and socio-economic work. It was devoted both to an analysis of the 2002 disaster and to more general climatological analyses of past and simulated future climate.

The present work presents one of the contributions to this project (called Startclim.4), dealing with the synoptic and regional patterns of heavy precipitation in Austria. Regional patterns of such events were sought primarily as an intermediate step for a robust identification of heavy precipitation events through areal precipitation means. Back trajectories computed for cases with observed heavy precipitation were grouped in order to identify synoptic patterns causing heavy precipitation events in Austria. This paves the way for automatic synoptic typing, relying solely on fields as provided by global meteorological models and thus applicable also to output of global climate simulation models. According to Yarnal (1993), this approach is an “environment-to-circulation” classification.

In both steps, clustering is applied to identify groups. A combined iterative-hierarchical clustering method has been developed which appears to be capable of combining the advantages of both base methods while eliminating their disadvantages. Stohl and Scheifinger (1994) already used

clustering of back trajectories to create synoptic patterns for Austria, which were mainly employed for looking at air pollution. They worked with a purely iterative algorithm.

The investigation of synoptic patterns (weather types) and their relationship to meteorological elements and other quantities has a long history, and only a selection of related work can be considered here. The standard method for Austria used by the meteorological service (ZAMG) is the classification of Lauscher (1972). More recently, Kerschner (1989) has created an Austrian version of the Swiss classification by Schüepp (1968). In Germany, the standard method is the one from Hess and Brezowsky (Hess and Brezowsky, 1977). Kerschner (1989) and Tveito and Ustrnul (2003) contain a lot of further references. Steinacker (1990) has created a classification for the Eastern Alps based on the flow direction in lower atmospheric levels which has also been widely used in Austria. None of these methods has all of the properties which we sought. Most importantly, they cannot be applied only on the basis of large-scale meteorological information as created by numerical weather prediction or general circulation models, as they contain elements of observed weather, subjective components, and/or rely on relatively small-scale features. Also, none of them includes the temporal dimension of the synoptic development, and none was specifically created for the analysis of heavy precipitation. Most of the classifications contain more than 20 classes, with the effect that some of them have such a small frequency that statistically stable applications are only possible by merging classes. A recent attempt to find an objective method that would allow to reproduce the Hess-Brezowsky classification automatically was not very successful (Schneider et al., 2003). Bissoli and Dittmann (2001) introduced an alternative, completely automatic classification system for the German Weather Service, which is made up of 40 classes defined by wind direction, cyclonic versus anticyclonic and wet versus dry conditions. A different approach, closer to our own one, has been followed by Plaut and Simonnet (2001) in the context of the ACCORD project (Atmospheric Circulation Classification and Regional Downscaling). They introduced an objective classification of weather regimes based on clustering truncated EOF representations of the 500 hPa and 700 hPa surfaces and the sea-level pressure, treated separately. Also this method does not consider the temporal development. Four or five regimes were obtained, which appear to be less sharp with respect to observed weather than more detailed classifications, including our own. Kyselý and Huth (2003) also developed a classification method based on clustering of EOF representations of 500 hPa surface heights, obtaining 14 to 17 clusters regrouped into 5 major types. In conclusion, the efforts in finding and applying synoptic classification schemes are presently moving from (semi-)subjective to automated or (quasi-)objective methods. Our approach seems to be a rather unique one.

Fricke (2003) looked into the relationship between the long-term evolution of the frequency of heavy precipitation and the Hess-Brezowsky weather types. The paper demonstrates that this classification is not separating the heavy-precipitation days well from other days.

A frame of reference for our results on the distribution of heavy precipitation for different synoptic

patterns is given by the already-mentioned work of Kerschner (1989) and his teacher Fliri (Fliri and Schüepf, 1984), who used the classification of Lauscher.

2 Data

2.1 Meteorological fields

The meteorological fields used for trajectory calculations were taken from ECMWF's 15-year reanalysis (ERA-15; Gibson et al., 1997), covering the years 1979-1993. Their horizontal resolution was 1° , and the lowest 28 out of the 31 vertical levels were used, excluding those above 100 hPa. The temporal resolution was 6 h. A sub-domain covering Europe and a part of the Atlantic Ocean (30°W – 50°E , 30°N – 70°N) was extracted. Fields of this resolution are available also for climate scenarios from time-slice simulation runs with a spectral resolution of T106. Thus, the methodology can be used in future applications for diagnosing simulated climates. The resolution is sufficient to resolve synoptic-scale features in the trajectories and thus for the desired synoptic classification.

2.2 Trajectories

Three-dimensional back trajectories were calculated with the FLEXTRA trajectory model (Stohl et al., 1995). The calculations were carried out for 8 receptor points in and around Austria at 8 arrival levels and for 8 arrival times each day. The trajectory positions were recorded each hour in the first two days before arrival and in 6 h intervals in the preceding two days (total trajectory length was 4 days). Specific humidity and potential vorticity (standard output of FLEXTRA) were written out in addition to the trajectory positions. This results in a total of about 12 GB of data (ASCII format, slightly modified compared to original FLEXTRA scheme to reduce the space). Obviously, this is much more information than needed to characterise the synoptic situations. As it was not known beforehand which data would be most important and how sparse they may be without loss of relevant information, we stored all of them and leave it to the evaluation to find the essential subset.

For the clustering, it is necessary to define a measure of similarity or dissimilarity (distance) between the trajectories belonging to one day. As explained, we aimed at using only a subset of the available information. Thus, this distance is made up by a variable set of contributions. These distance elements are the horizontal and the vertical position distance along a given segment of a single trajectory, and the distance in the specific humidity or the potential vorticity which was considered only upon arrival. The segments considered are 0–24 h, 24–48 h, and 48–96 h before arrival. The distance measure for the horizontal distance is

$$d_{xy}(k, l) = \frac{1}{N} \sum_{i=1}^N (\sigma_{x_i}^{-1} |x_i(k) - x_i(l)| + \sigma_{y_i}^{-1} |y_i(k) - y_i(l)|) \quad (1)$$

where k and l denote the two trajectories to be compared, and the index i enumerates the data points within each segment. Coordinates x and y as well as their standard deviations are in degree longitude and latitude. The standard deviations σ_x and σ_y were calculated from a large subset of the total trajectory data set. They are specific to a trajectory arrival level and depend on the time along the trajectory (index i). The other distances are simpler and calculated analogously.

2.3 Precipitation data

Diurnal precipitation sums of 132 climate stations of the Austrian national meteorological service (ZAMG) during the ERA-15 period (1979-1993) were available. Data had been quality-controlled by another Startclim project contribution (Formayer et al., 2003). Of these, one station was immediately discarded because of a very short series of available data. Among the remaining 131 stations, four stations had less than ten years of data, and another 16 stations less than 14 years. The stations cover the whole territory of Austria and include a number of mountain stations. They were clustered into regions to exclude local-scale events (see Section 4). The station list is available in our full report (Frank and Seibert, 2003).

3 Clustering method

The clustering method best established for trajectories is the iterative method introduced by Dorling and Davies (1992), which is often called “K-mean” method in the statistical literature. A number of so-called seed trajectories, corresponding to the number of clusters desired, is defined either as an arbitrary subset of the trajectory data set or as artificial trajectories, e.g. from different directions. Trajectories are assigned to the clusters (in the beginning consisting only of the seed trajectory) to which they are closest. This is determined by the distance of the respective trajectory to the arithmetic mean of all elements of a cluster. As the (re)assignment modifies the cluster, the procedure is iterated until a stable solution is obtained. However, it can be shown that the choice of the seed trajectories (or elements, as this procedure is not specific to trajectories) can influence the result (Krishnaiah and Kanal, 1982). The advantage of this method is that even for large data sets the computational demands are moderate.

The most popular general clustering method is hierarchical clustering (Anderberg, 1973). There is a top-down and a bottom-up variant. In the latter, each element forms its own cluster at the beginning. Then, the two clusters which are closest to each other are joined. This is repeated until all the elements are in one cluster. The top-down method works vice versa. As in the iterative method,

one has to decide how many clusters are considered appropriate. Whereas in the iterative method this is completely arbitrary, the hierarchical method offers the series of (dis-)similarity measures between the two clusters joined (split) in each step as a guidance. If (in the bottom-up case) a sudden decrease in the similarity is found, this is obviously the step where the process should be terminated. The hierarchical method can be used with different so-called linkage methods. We used the average-linkage method. In this case, the mean value of the distances of each cluster element to the elements of another cluster is defining the distance between these two clusters. A half-matrix of the distances (similarities) between all elements is used as input in this method.

An obvious disadvantage of the hierarchical clustering is that once an element is assigned to one cluster, it cannot be reassigned to another cluster, in spite of the fact that the shape of the different clusters is changing throughout the clustering process. Therefore, we decided to combine the rearrangement as in the iterative method with the hierarchical method. In a first attempt, rearrangement was carried out after the completion of the hierarchical clustering, at the desired number of clusters. This method was used here to form the precipitation regions. Working with clustering of the trajectories, we felt that using the distance to the average of all elements is not satisfactory. A well-known saying in statistics is that the average is the value that is never found in the data. This can lead to clusters where there is no preferred wind direction. In this case, the average trajectory has lower speed than any typical element of the trajectory set, and its direction is ill-defined. Therefore we decided to replace the average element by the so-called central element. The central element in our approach is defined as the one having the smallest average of the distances to all other elements in its cluster. A very welcome by-product of this modification is that it is no more necessary to read in again all trajectory coordinates of a cluster to calculate the average and to calculate the distances between it and each of the elements. The whole process is based upon the pre-calculated distance matrix. For large data sets, especially with a large size of each element, this is a substantial advantage. As a later improvement, the rearrangement after each step of the hierarchical clustering was introduced, which is a more natural way. The clustering of trajectories was done with this method.

Summarising, our combined method avoids the problem of the influence of the choice of the seed elements in the iterative (K-mean) approach, and it enables a more objective determination of the cluster number like in the hierarchical clustering while avoiding the problem in this latter approach that an element is fixed in a cluster through the procedure. Furthermore, by replacing the mean element with the central element in the rearrangement, it makes the procedure computationally more efficient and presumably gives more meaningful results in those situations where the mean is not similar to any cluster member.

We used the CLUSBAS Fortran programme of John S. Uebersax in the STATLIB free software collection (<http://lib.stat.cmu.edu/general/hcxfb>) as the basis, adding to it the rearrangement. Our

new combined clustering method is available for download.¹

4 Precipitation

4.1 Regional clustering

A clustering of all precipitation stations was performed with the algorithm described above. The basis was a similarity matrix, and the similarity measure for a station pair was the squared correlation coefficient between the time series of diurnal precipitation at these stations. This is a quadratic measure, so that the similarity is strongly influenced by strong precipitation events. This was desired for our purpose of investigating heavy precipitation.

4.2 Regional patterns

According to the similarity measure series of the clustering steps and an a-priori idea of the order of magnitude of the number of clusters, seven regions with similar time series of the daily precipitation sums were obtained. For the following discussions some knowledge of the Austrian topography is required. Figure 1 provides an overview and helps to understand the central role played by the Alps for the Austrian climatic provinces.

Figure 2 shows these regions for the whole year, for the summer and for the winter half years, respectively. They are discussed in the order West–Northeast–South for the full year, followed by an outline of the variations found for both summer and winter.

The West region (Vorarlberg and most of Northern Tyrol) forms the first region. The second region has been termed “Northern Stau” region. It covers the areas north of the Alpine main ridge in the state of Salzburg, the lower parts of the state of Upper Austria, and the easternmost stations of North Tyrol. The third region consists mainly of the elevated regions in the North of Austria, called “Wald- and Muehlviertel”. Eastern Austria, with Vienna as its centre and including the northern part of Burgenland with the Neusiedl lake, forms the fourth region, called “East region”. The climate of this regions is sometimes described as “pannonian” (similar to adjacent Hungarian plains). Interestingly, it reaches westward beyond the so-called Vienna Woods, the eastern tail of the Alps, though they are often conceived as a climatic divide. A smaller cluster is recognised along the northern edge of the eastern part of the Austrian Alps. It comprises a strip from Enns Valley to the Rax-Semmering region and is called here Ennstal-Semmering region. Most of Styria, eastern (lower) Carinthia, the southern Burgenland and the Lungau (a small part of Salzburg south of the main Alpine divide) form another cluster termed “South-east region”. It is also known to

¹<http://www.wau.boku.ac.at/2393.html&&L=1>

have a distinct climate. The last region is made up of East Tyrol and western (upper) Carinthia, south of the Alpine main ridge, which we term “Southern Stau” region because it is characterised by heavy precipitation with southerly flows.

The regions found for the summer half year are relatively similar to those of the whole year. The East region is smallest in this time of the year and coincides with its orographic definition. The Enns Valley joins the Northern Stau region, whereas the Rax-Semmering regions is joined with the mountains to the East (Wechsel region), known for heavy thunderstorms in the warm season. The Southern Stau region is smallest in the summer half year. On the other hand, it grows in winter when it includes also two stations in West region which are very close to the Alpine main ridge, Obergurgl and Brenner. This corresponds to the well-known fact that precipitation caused by southerly “Stau” is most intense and frequent in autumn and winter, and often still affects areas north of the main ridge. The station Boeckstein-Mallnitz in Salzburg has a similar orographic situation and is part of the Southern Stau region throughout the year. The Northern Stau region comprises the whole eastern part of North Tyrol in the winter half year as well as the Enns Valley, whereas the northern parts of the region are split off. They merge with the western part of the Wald- and Muehlviertel region (Muehlviertel). The eastern part (Waldviertel) joins the East region.

If it is considered how well each station is correlated with the others of its clusters, it can be detected that some border stations do not fit in very well. Thus, if the study had taken into account a larger area, not limited to the territory of Austria, we would probably see more clusters, with some Austrian stations belonging to them. We can also recognise the well-known fact that the spatial correlation of precipitation is higher in winter than in summer.

Matulla et al. (2003) have also divided Austria into precipitation regions by statistical means. However, they were analysing year-to-year variations of mean monthly precipitation data, whose spatial patterns do not need to coincide with those related to day-to-day variations as studied in this paper. Furthermore, they used only 31 stations, and about 100 values per station (as compared to about 5000 values in this paper), making it more difficult to resolve smaller regions. Nevertheless, the three major subdivisions (western, southern, and northeastern parts of the country) found by them are in basic agreement with the subdivisions found by us for the synoptic precipitation patterns.

4.3 Precipitation amounts

As a basis for the subsequent identification of synoptic patterns connected to heavy precipitation, such heavy precipitation days had to be identified. We did not want to do this on the single-station level, as isolated thunderstorms whose exact location is hardly predictable might affect the result too much. Also, as we want to look at relatively rare events, it is necessary to use a statistically robust property. Therefore regional means of the precipitation in the regions described above were

used. For each region, an estimate of the mean regional precipitation was obtained as the average of station values.

Some percentiles of the precipitation distribution in the seven regions are given in Table 1. The 98th percentile has been used as a criterion for heavy precipitation days, i.e., a day is considered a heavy precipitation day for Austria if the mean precipitation exceeds the respective 98th percentile in at least one region. This criterion yields 400 days in the 15 years of our data set. In the majority of regions, the 98th percentile is about 20 mm/d. In the Southern Stau region, it is higher (27 mm/d), and in the East and North regions, it is lower (14 and 13 mm/d). The highest value of the mean regional precipitation in the 15-year time series as well as the ratio between this maximum and the 98th percentile is also given. This ratio is an indication of the elongation of the tail of the distribution. It varies between 2.6 and 3.7 for all regions except the East region where it takes the value 5.5. This is also reflected in the fact that while this region is the driest in all percentiles up to the 98th, it comes third in the maximum, almost the same value as in the South-east region. This indicates that the East region has a potential for quite rare but rather strong heavy-precipitation events.

The criterion of the 98th percentile can also be applied to each region separately, and the resulting annual variation of the number of days exceeding the (whole-year) 98th percentile is presented in Table 2. Most of the regions have a very pronounced summer maximum. For the Southern Stau region, the autumn maximum which is typical for the southern side of the Alps is found in October. The South-east region has at least a secondary maximum in this month, and the East region has its maximum in September (in addition to a secondary maximum in May and June). Regions influenced by northerly “Stau” (Northern Stau region, West region, Ennstal-Semmering region) have a pronounced secondary maximum in winter, varying between December and February/March.

5 Synoptic patterns

5.1 Trajectory clustering

Clustering of trajectories was performed only for those days which were diagnosed as heavy precipitation days. This limited the computer requirements and allowed us to play around with many different combinations of information (different levels and times of arrival of the trajectories and different physical quantities). In addition, we used a subset of 676 days from the remainder of the data set, selected randomly but matching the number of occurrences per month as closely as possible. These days served to check how specific the clusters are to heavy precipitation.

While considering the vertical position (and thus vertical motion) and the specific humidity in the distance matrix for clustering resulted in a good separation of heavy precipitation and other days,

it prevented clusters from reflecting specific flow patterns, as rising moist air is likely to lead to precipitation, whether it comes from the southwest or the northwest. Considering the background of the project—development of a diagnostic tool for climate scenario runs—we found it more important to identify distinct synoptic patterns than having a good decision algorithm, especially given the fact that the synoptic patterns can be expected to be more robust in climate scenarios than vertical motion fields.

Therefore we tested systematically which horizontal positions in the distance measure for clustering would yield the best separation between strong precipitation days and others, expressed by the overlapping area below the cumulative frequency distributions. We started at one arrival point in the northwest of Austria at the bottom level and combined the horizontal position of this trajectory with the horizontal position of the other trajectories ending at that point at the same time but on higher levels. Next, we combined each level with each other level at this point and time and calculated the overlapping area as skill score. Using only the trajectories ending at this point and time, a combination of level 2 and level 7 yields the smallest area. Taking a third arrival level into account made the result worse. Keeping level 2 and 7 at point Northwest and time 16:30 UTC, we tested contributions from all other arrival points in Austria, including trajectories arriving at other levels and times during the day. We ended up with the combination of distance measures described in Table 3. This information from nine different trajectories includes different height levels of arrival, different arrival points in Austria and different times of arrival during the day.

Only the trajectory segment covering the 24 h before arrival was taken into account because, when playing around with different combinations of distance contributions, we had the impression that trajectory differences longer back are not so relevant for the weather on the arrival day. The lower level (arrival 500 m agl) received a higher overall weight as more arrival times are used at this level. The usage of different arrival times is a means of representing the phase speed of weather systems, and considers at least to some extent that precipitation events are of course not necessarily centred on a 07-07 LST observation day. Similar considerations hold for using two arrival grid points. The effects of in-stationarity are in addition contained in the trajectories themselves, as they move through time. Positions were also used at a mid-tropospheric level (arrival 500 hPa). Using different levels allows to take into account wind shear and thus also temperature advection in an implicit way. The potential vorticity also enters the distance measure because it can be useful to distinguish cyclonic situations. Potential vorticity is provided as a part of the standard FLEXTRA output. In the future, we would like to check if relative vorticity would be a better parameter.

This distance function led to eight clusters for heavy precipitation days. One of them consisted of one single day only (with high wind speeds) which is skipped for the statistical analyses.

5.2 Resulting synoptic patterns

In Fig. 3, each cluster is presented by a plot of all trajectories arriving at the near-ground and the mid-tropospheric level belonging to this cluster, for one arrival point and time.

Pattern 1 is a typical southerly “Stau” and occurs in 20% of all of the 400 selected days with heavy precipitation in Austria. It is characterised by a moderate southerly flow at higher levels as well as near ground. Most of the ground-level trajectories stayed some time over the Mediterranean Sea and took up humidity which is subsequently rained out in the southerly “Stau” of the Alps.

Pattern 2 is a quite different type. Very slow movement near ground (mean speed within the last 24 hours 3.8 m/s) indicates situations with weak pressure gradient. At higher levels, a well-pronounced, not too fast southwesterly flow prevails. Precipitation in this pattern is mainly convective, and includes pre-frontal storms and summerly cold-front passages. Correspondingly, this pattern can cause heavy precipitation everywhere in Austria and therefore it is relatively frequent (47% of the cases). Because it contains mainly convective events, it has a pronounced seasonal cycle: 59% fall into the three summer months, less than 2% into the winter, and each about 15% into spring and autumn. The (relatively few) winter and autumn cases appear to be synoptically different, being characterised by upgliding of warm air from the south-east or east. This indicates a certain weakness of the present clustering, and adding a stability index should be considered in the future.

The algorithm identified three patterns with northwesterly flow. Pattern 3 is the most frequent one of them (11% of all cases). The ground level trajectories stay a long time over the Atlantic Ocean, thus enabling a strong humidification of the air. Apart from the convective pattern 2, this is the most frequent cause of heavy precipitation days north of the Alps. The two other patterns with northwesterly flow (patterns 4 and 5) show much higher wind speeds at ground level as well as at higher levels. In Pattern 4 (2% of all cases) the ground-level trajectories come directly from the west. This causes heavy precipitation in the west of Austria (westerly “Stau” effect). Pattern 5 (3% of all cases) shows a strong northwesterly flow at both levels, and has a pronounced northerly component at higher levels. Especially orographically enhanced lifting of warm air causes heavy precipitation events in Northern Stau areas in this pattern. According to synoptic experience, this pattern can be associated with warm-front waves.

Pattern 6 is characterised by a cut-off low in the region east of Austria. A well-developed low-pressure system at higher levels in the (north-) east of Austria causes cold-air advection at its back. This cold air inflow at higher levels destabilises the air and thus is conducive to precipitation. In the northern Stau regions, this effect is enhanced by forced uplifting of the air and produces high amounts of precipitation. This weather pattern was found in 4.5% of all cases.

As the seventh pattern, the algorithm identified the so-called Vb situation. In this situation, which

accounts for 12% of all cases, a low develops south of the Alps and then moves towards the northeast. These situations are often connected with heavy precipitation because the air which is lifted in the depression has taken up a lot of humidity over the Adriatic Sea, and because the systems move relatively slowly. Relatively low wind speeds at both levels corroborate that. Typical is also the inflow of cold air from the north near ground which is the reason why this pattern can cause heavy winter storms in the east of Austria. Nearly all of the ground-level trajectories show these northerly directions. The upper level trajectories show the typical inflow of humid air in the east of Austria. Not the whole of a Vb development, typically lasting several days, is contained in this pattern. The early stages of Vb developments may be classified as the southerly Stau pattern 2, and some of them may transform into a pattern-6 type with a cut-off low (the classical Vb situation is connected with a sharp trough).

5.3 Precipitation distribution for the synoptic patterns

In order to characterise and compare the associated precipitation amounts, the spatial distribution of precipitation in Austria for the seven weather patterns was investigated. The median of the daily precipitation of all heavy precipitation days was calculated for each station in Austria and for each weather pattern. These values were interpolated in a GIS with the Kriging method and the resulting spatial distributions are shown on maps in Figure 4. Here we should also keep in mind that extreme situations are usually caused by events with two or more consecutive days with heavy precipitation. Our analysis, however, is limited to separate consideration of each day.

Pattern 1 causes heavy precipitation almost exclusively in the Southern Stau region (median values up to more than 50 mm) while there is no or little precipitation north of the Alps. Pattern 2 can bring heavy precipitation all over the country, with a minimum of the intensity in the north-east. The most frequent one of the northwesterly flow patterns, pattern 3, brings high precipitation values primarily to the Northern Stau regions. Pattern 4 exhibits a westerly “Stau” effect as visible by the maximum in the Arlberg region. Most affected by pattern 5 is the Northern Stau region, similar to pattern 3, but with lower amounts in the extreme west and clearly higher ones in the Enns Valley (median reaches 40 mm/d). Pattern 6, identified as cut-off low in the east, causes the most intense precipitation events in the typical northerly “Stau” regions. Pattern 7, the so-called Vb type, causes the highest amounts of precipitation in the north-east of Austria and the eastern part of the Northern Stau region. Daily precipitation values exceed 20 mm, which is quite a lot for the rather dry East region (and the weather pattern can persist for more than one day!). Next to pattern 2, the Vb pattern is the second most important one for heavy precipitation in southern Styria.

One should keep in mind that the median does not represent the highest possible daily sums, which are typically higher by a factor 2 to 3. The Southern “Stau” region has the highest maximum values

with daily precipitation reaching amounts about 80 mm in the regional mean. At single stations, 24-hour precipitation reached as much as 205 mm at Loibl, 162 mm at Kornat or 159 mm at Reisach (all in the southwest of Austria).

5.4 Relationship between synoptic patterns and regions

In addition to Figure 4, Table 4 illustrates how synoptic patterns are linked to the regions with respect to heavy precipitation events. For patterns 4 to 6, the low absolute number of occurrence and thus the statistical uncertainty of the results has to be taken into account.

Pattern 1, southerly flow, has a high probability of causing heavy precipitation only in the Southern Stau region, and it is the only pattern there with a high probability. Interestingly, the southerly “Stau” pattern comes out as relatively important also for the West region, accounting for about 20% of the events there, though nearly the whole region lies north of the main alpine crest. In many cases of cyclonic southerly flow, the cold front is positioned east of the region, and wave induction over the Alps and Northern Italy can cause upglide precipitation which reaches towards the north over the main Alpine crest. Stations close to the main ridge can also be affected by the advection of precipitation particles during their fall (Zängl, 2005), an effect described already in Section 4.2.

The heavy-precipitation probability for the weak-gradient situation, pattern 2, is distributed rather homogeneously over Austria, as expected. It has a maximum for the South-east region where this pattern is also the most relevant one. This is probably linked to the fact that pattern 2 is often associated with weak southerly or southwesterly flow. This pattern 2 is the most frequent cause of heavy precipitation events in absolute numbers everywhere except the Southern Stau region. This is due to high absolute incidence of this situation among all the heavy-precipitation days, linked to the fact that it occurs mainly in the warm season where precipitation amounts are generally higher.

The typical northwesterly flow pattern (number 3) is most effective in the Northern Stau region. The westerly flow situation (number 4) is most probable to cause heavy precipitation in the West region. Finally, the NNW pattern (number 5) is likely to be associated with heavy precipitation in the Ennstal-Semmering, the Northern Stau and the West regions. Everywhere else this pattern has a very low likelihood of such events. This discerns it from the two other patterns associated with flow from the NW quadrant.

Synoptic pattern 6, which is often characterised by a cut-off low to the east of Austria and thus a northerly flow, can affect all the northeast of Austria (Northern Stau, Wald- and Muehlviertel, East region, Ennstal-Semmering). It is most effective in the Ennstal-Semmering region, like the NNW pattern 5, indicating that the northern edge of the eastern part of the Alpine ridge is especially sensitive to stau effects caused by northerly flows. Contrary to pattern 5, it has no effect in the

West region, and it does have an effect in the Wald- and Muehlviertel as well as the East region.

The Vb situation (pattern 7) emerges as the second-most important cause of heavy precipitation events in northern and eastern Austria (Wald- and Muehlviertel region, where it is most effective, and East region) which corresponds to our synoptic experience. The fact that the Southern Stau region is not affected by this pattern, and the Southeast region only moderately, underlines the fact that this pattern identifies the phase of a Vb development where the surface low is already east of Austria, the previous stage falling into pattern 1.

Interestingly, the regions affected by patterns 6 and 7 coincide with those most affected by the extreme flood event in August 2002, in agreement with synoptic analysis of these events (Seibert and Formayer, 2003; Seibert et al., 2003).

6 Conclusions

A method has been derived and introduced to characterise synoptic patterns which can cause heavy precipitation events in Austria. The method is based on backward trajectories from several points in Austria, several times of the day and on multiple levels. Weather situations have been identified which correspond to the synoptic experience. The method can be used with NWP or GCM data as input.

As a by-product, a new cluster algorithm has been designed. It is based on a hierarchical iterative cluster method with average linkage, combined with rearrangement after each step based on a 'central' trajectory.

In a first step, Austria was partitioned into seven regions with similar occurrence of heavy precipitation by the cluster algorithm: West region, Northern Stau region, Wald- and Muehlviertel region, East region, Ennstal-Semmering region, South-east region and Southern Stau region.

The distance measure which was found to be best for the synoptic pattern clustering is a combination of the horizontal distance within the last 24 hours of the trajectories near ground and in the mid troposphere, at different arrival points and different times of the day, plus a measure of the vorticity upon arrival. The seven synoptic patterns identified for the heavy-precipitation days in Austria are: southerly "Stau", weak-gradient situation, northwesterly flow at all levels, westerly "Stau", fast northwesterly flow with upper-level northerly winds, upper-level low in the East, Vb situation. Characteristic distributions of heavy precipitation were found for each of these situations.

The results obtained give interesting insights into the synoptic climatology of heavy precipitation in Austria. The precipitation regions and the spatial distribution of heavy precipitation for the synoptic patterns could be a useful background information for catastrophe management or-

ganisation, as it shows which regions can be expected to be hit together under different synoptic circumstances. However, for classifying the heavy-precipitation potential of any given meteorological situation, a decision algorithm is desirable which includes not only a partitioning of different heavy precipitation situations, but also between those and situations without heavy precipitation. First results obtained for this decision within Startclim.4 are not yet satisfactory. It might be useful to extend the clustering procedure to cases without heavy precipitation, to introduce a third class of days with moderate precipitation (instead of lumping together all cases below the 98th percentile), or to introduce other distance measures as discussed in Section 3.

Acknowledgements

Helga Kromp-Kolb (Institute of Meteorology, BOKU Vienna) carried a large share of the burden to organise the large, heterogeneous Startclim project and opened the opportunity for us to perform this study. This project was supported financially by the Austrian Federal Ministry of Agriculture, Forestry, Environment and Water Management, The Federal Ministry of Education, Science and Culture, the Austrian Hail Insurance company, the Austrian National Bank, and the the Federal Environment Agency. The climate station data were kindly made available by the Austrian Meteorological Service ZAMG, and ECMWF data were accessible through our Special Project SPATMOT. Caroline Forster and Sabine Eckhardt (Technical University of Munich) made available to us their tapes with extracted ERA-15 data. Paul James and Andreas Stohl from the TU Munich group provided some inspiration to this work by their yet unpublished trajectory analysis of the August 2002 flood in Germany.

References

- Anderberg MR (1973) Cluster analysis for applications. Probability and Mathematical Statistics. New York: Academic Press. 359 pp.
- Becker A, Grunewald U (2003) Flood risk in Central Europe. *Science* 300(5622):1099
- Bissoli P, Dittmann E (2001) The objective weather type classification of the German Weather Service and its possibilities of application to environmental and meteorological investigations. *Meteorologische Zeitschrift* 10:253–260
- Dorling S, Davies T (1992) Cluster analysis: A technique for estimating the synoptic meteorological controls on air and precipitation chemistry—method and applications. *Atmospheric Environment* 26A:2575–2581
- Fliri F, Schuepp M (1984) Synoptische Klimatographie der Alpen zwischen Mont Blanc und Hohen Tauern und alpine Witterungslagen und europäische Luftdruckverteilung, vol. 29 of *Wissenschaftliche Alpenvereinshefte*. Innsbruck, Austria
- Formayer H, Matulla C, Haas P, Groll N (2003) Statistische Downscalingverfahren zur Ableitung von Extremereignissen in Österreich. In: H Kromp-Kolb, I Schwarzl (eds.), *Startprojekt Klimaschutz:*

- Erste Analysen extremer Wetterereignisse und ihre Auswirkungen in Österreich. Endbericht.* Vienna: Institut für Meteorologie und Physik, Univ. für Bodenkultur Wien. Band 1, 5.1-5.22, on-line at <http://www.austroclim.at/startclim/>
- Frank A, Seibert P (2003) Diagnose von Extremereignissen aus großräumigen meteorologischen Feldern. Endbericht zum Projekt StartClim.4. In: H Kromp-Kolb, I Schwarzl (eds.), *Startprojekt Klimaschutz: Erste Analysen extremer Wetterereignisse und ihre Auswirkungen in Österreich. Endbericht.* Vienna: Institut für Meteorologie und Physik, Univ. für Bodenkultur Wien. Band 1, 4.1-4.44, on-line at <http://www.austroclim.at/startclim/>
- Fricke W (2003) Sind veränderte Wetterlagen die Ursache für zunehmende Starkniederschläge in Deutschland? In: *6. Deutsche Klimatagung, Potsdam*, pp. 150–154. Alfred-Wegener-Stiftung
- Gibson JK, Kallberg P, Uppala S, Nomura A, Hernandez A, Serrano E (1997) ERA Description. ECMWF Reanalysis Project Report Series No. 1, 72 pp.
- Hess P, Brezowsky H (1977) Katalog der Großwetterlagen Europas 1881-1976. Offenbach/Main, Germany
- Kerschner H (1989) Beiträge zur synoptischen Klimatologie der Alpen zwischen Innsbruck und dem Alpenostrand. No. 17 in *Innsbrucker Geographische Studien*. Innsbruck: Institut für Geographie der Universität Innsbruck. 253 pp.
- Krishnaiah PR, Kanal LN (eds.) (1982) Classification, pattern recognition and reduction of dimensionality. *Handbook of Statistics*. Amsterdam: Elsevier Science Publishers. 903 pp.
- Kromp-Kolb H, Schwarzl I (eds.) (2003) *Startprojekt Klimaschutz: Erste Analysen extremer Wetterereignisse und ihre Auswirkungen in Österreich. Endbericht.* Vienna: Institut für Meteorologie und Physik, Univ. für Bodenkultur Wien. <http://www.austroclim.at/startclim/>
- Kubát J, Šercl P, Coufal L (2003) Preliminary summary report on hydrometeorological situation during the August 2002 fbods. Czech Hydrometeorological Institute, Praha, Czech Republic, 16 pp., on-line at <http://www.chmi.cz/hydro/pov02/fbod.htm>
- Kyselý J, Huth R (2003) Recent changes in atmospheric circulation over Europe detected by objective and subjective methods. In: *Preprints 14th Symposium on Global Change and Climate Variations*. Amer. Meteor. Soc. paper P3.1, on-line at http://ams.confex.com/ams/annual2003/techprogram/paper_54197.htm
- Lauscher F (1972) 25 Jahre mit täglicher Klassifikation der Wetterlage in den Ostalpenländern. *Wetter und Leben* 101:185–189
- Matulla C, Penlap EK, Haas P, Formayer H (2003) Multivariate techniques to analyse precipitation in Austria during the 20th century. *International Journal of Climatology* 23:1577–1588
- Plaut G, Simonnet E (2001) Large-scale circulation classification, weather regimes, and local climate over France, the Alps and Western Europe. *Climate Research* 10:303–324
- Schneider F, Enke W, Deutschländer T (2003) Eine Objektivierungsmethode für die Großwetterlagen nach Hess & Brezowsky. In: *6. Deutsche Klimatagung, Potsdam*, pp. 380–384. Alfred-Wegener-Stiftung

- Schüepp M (1968) Kalender der Wetter- und Witterungslagen von 1955 bis 1967 im zentralen Alpengebiet, vol. 11 of *Veröffentlichungen der SMA*. Zürich, Switzerland
- Seibert P, Formayer H (2003) Meteorologische Situation. In: H Habersack, A Moser (eds.), *Ereignisdokumentation Hochwasser August 2002*, pp. 17–22. Vienna: Universität für Bodenkultur Wien, <http://zenar.boku.ac.at/PDF-Files/Hochwasser'2002'Gesamt.PDF>
- Seibert P, Formayer H, Habersack H (2003) Niederschlag. In: H Habersack, A Moser (eds.), *Ereignisdokumentation Hochwasser August 2002*, pp. 23–26. Vienna: Universität für Bodenkultur Wien, <http://zenar.boku.ac.at/PDF-Files/Hochwasser'2002'Gesamt.PDF>
- Steinacker R (1990) Eine ostalpine Strömungslagenklassifikation. Institut für Meteorologie und Geophysik, Universität Wien (previously: Universität Innsbruck), Austria, <http://www.univie.ac.at/IMG-Wien/weatherregime/>. 8 pp.
- Stohl A, Scheifinger H (1994) A weather pattern classification by trajectory clustering. *Meteorologische Zeitschrift* 3 (N.F.)(6):333–336
- Stohl A, Wotawa G, Seibert P, Kromp-Kolb H (1995) Interpolation errors in wind fields as a function of spatial and temporal resolution and their impact on different types of kinematic trajectories. *Journal of Applied Meteorology* 34:2149–2165
- Tveito OE, Ustrnul Z (2003) A review of the use of large-scale atmospheric circulation classification in spatial climatology. DNMI Report 10/03 KLIMA, ISSN 0805-9918, on-line at <http://cost719.met.no/papers/CP-methods.pdf>, Blindern, Norway. 17 pp.
- Yarnal B (1993) Synoptic climatology in environmental analysis. *Studies in Climatology Series*. London: Belhaven Press. 195 pp.
- Z'angl G (2005) The impact of lee-side static stability on the distribution of orographic precipitation. In: *Croatian Meteorological Journal*, vol. 40, pp. 57–60. 28th International Conference on Alpine Meteorology (ICAM), Zagreb: Croatian Meteorological Society

Address for correspondence: Dr. Petra Seibert, Institut für Meteorologie der Universität für Bodenkultur Wien, Peter-Jordan-Str. 82, 1190 Wien, Austria.

Tables

Table 1: Percentile values [mm/d] of the mean regional daily precipitation for the seven precipitation regions of Austria. The last column contains the ratio between the maximum regional precipitation value and the 98th percentile. Based on period 1979 – 1993 (5479 days).

Region	P e r c e n t i l e							p100/p98
	25.0	50.0	75.0	90.0	95.0	98.0	100.0	
1 West region	0.0	0.6	4.0	9.6	14.4	21.2	65.8	3.1
2 Northern Stau region	0.0	0.9	4.8	10.4	15.2	20.8	62.5	3.0
3 W/M-viertel region	0.0	0.3	2.2	5.9	9.1	13.9	51.0	3.7
4 East region	0.0	0.1	1.5	4.9	8.2	12.9	70.5	5.5
5 Ennstal-Semmering region	0.0	0.5	3.5	9.4	14.3	21.7	56.2	2.6
6 South-east region	0.0	0.2	2.1	7.4	12.5	20.7	70.7	3.4
7 Southern Stau region	0.0	0.3	2.7	9.2	16.0	27.3	82.2	3.0

Table 2: Number of days per month and region exceeding the (whole-year) 98th percentile in the 15 years 1979-1993. Row-wise maxima are printed in bold and secondary maxima are starred (*), row-wise minima are underlined.

Region	M o n t h											
	1	2	3	4	5	6	7	8	9	10	11	12
1 West region	6	*7	*7	<u>2</u>	4	21	18	17	12	4	6	5
2 Northern Stau region	6	3	4	<u>1</u>	9	16	21	17	10	6	6	*10
3 W/M-Viertel region	<u>1</u>	2	5	9	18	21	18	14	11	3	*5	2
4 East region	<u>1</u>	3	8	7	*14	*14	11	13	16	6	8	6
5 Ennstal-Semmering region	*8	<u>4</u>	5	<u>4</u>	7	11	15	20	12	12	5	7
6 South-east region	<u>1</u>	3	2	2	9	13	16	18	15	*16	12	3
7 Southern Stau region	<u>2</u>	5	6	6	*9	6	12	11	13	19	12	9

Table 3: Final combination of trajectory data used in the distance measure for the clustering of weather patterns. hor. pos. means horizontal position, pot. vort. potential vorticity. See text for explanation of arrival points. Arrival time of 04:30 refers to following day as 07-07 LST precipitation data are used.

trajectory parameter	arrival level	arrival point	arrival time (UTC)
hor. pos.	level 2 (500 m agl)	Northwest	16:30
hor. pos.	level 2 (500 m agl)	Southeast	16:30
hor. pos.	level 2 (500 m agl)	Northwest	07:30
hor. pos.	level 2 (500 m agl)	Southeast	07:30
hor. pos.	level 2 (500 m agl)	Northwest	04:30
hor. pos.	level 2 (500 m agl)	Southeast	04:30
hor. pos.	level 7 (500 hPa)	Northwest	16:30
hor. pos.	level 7 (500 hPa)	Southeast	16:30
pot. vort.	level 6 (3000 m agl)	Northeast	16:30

Table 4: Probability in % that a day which is a heavy-precipitation day anywhere in Austria is associated with heavy precipitation in each region, as a function of the synoptic pattern. Bold numbers indicate which regions are most affected by a given synoptic type, whereas stars mark the synoptic type which results in the highest probability of heavy precipitation in a given region. The last line repeats the number of cases for each synoptic pattern. These patterns are labelled by their number and a short abbreviation found also in Figure 3.

Region	Synoptic pattern						
	1	2	3	4	5	6	7
	S	WG	NW	W	NNW	CL	Vb
1 West region	27	27	43	*78	67	0	10
2 Northern Stau region	10	31	50	33	*67	39	18
3 W/M-viertel region	5	33	11	44	8	28	*57
4 East region	19	31	23	11	0	22	*51
5 Ennstal-Semmering region	16	25	32	11	*83	50	29
6 South-east region	27	*37	14	0	0	6	18
7 Southern Stau region	*74	23	11	0	8	6	2
N	81	186	44	9	12	18	49

Figures

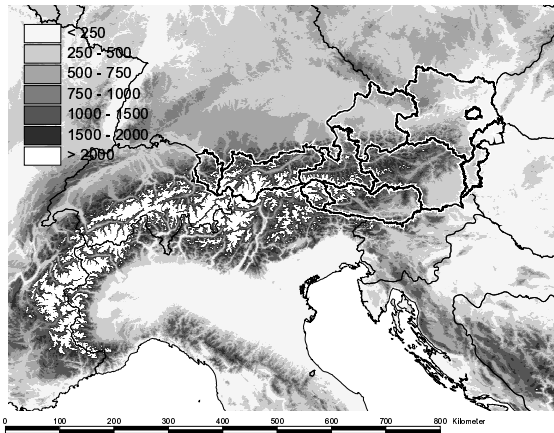
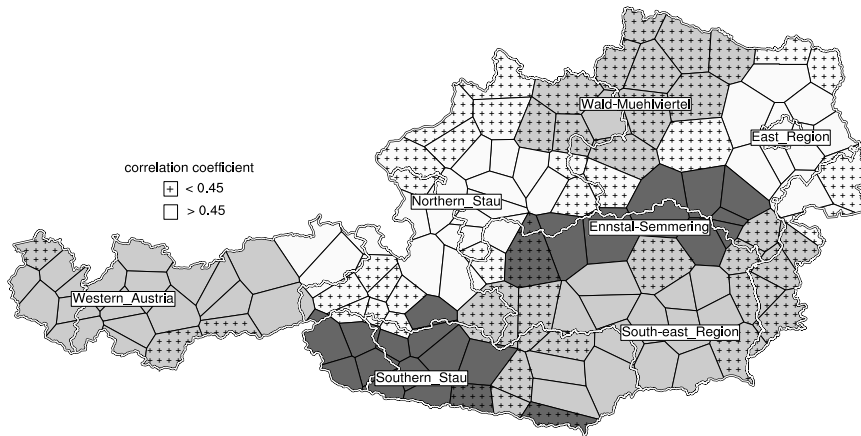
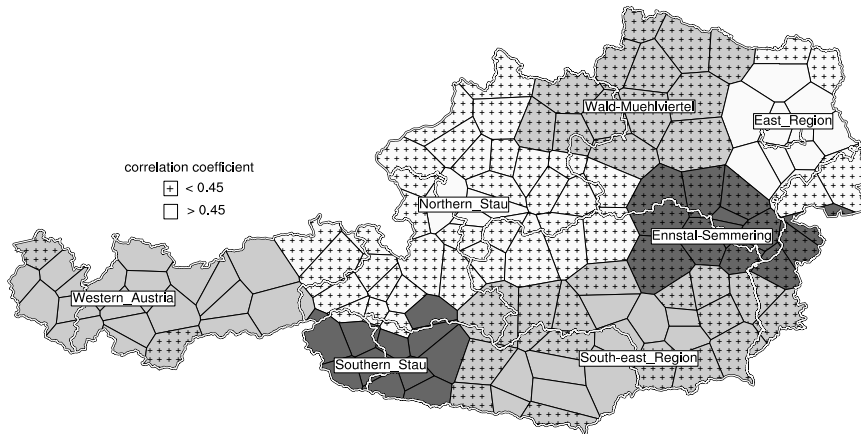


Figure 1: Topography of the Alps with Austria. Heavy lines denote the borders of the Austrian federal states (in clockwise direction, starting from the west: Vorarlberg, Tyrol, Salzburg, Upper Austria, Lower Austria, Vienna, Burgenland, Styria, Carinthia). Thin lines denote other international borders. Height of terrain in metres.

(a) Year



(b) Summer half-year



(c) Winter half-year

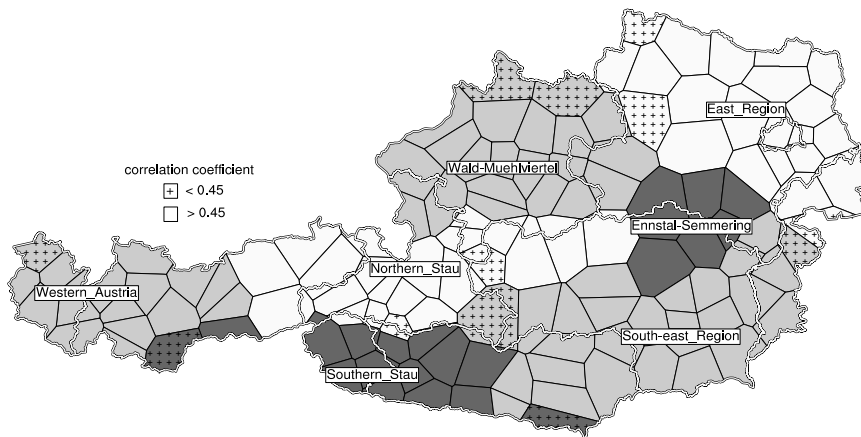


Figure 2: Seven precipitation regions of Austria, (a) whole year, (b) summer half-year, (c) winter half-year. The precipitation regions are indicated by grey shading. The correlation class for each station is indicated by hatching of the area around it (Thyssen polygon) with different symbols. The double lines mark the borders of the federal states of Austria.

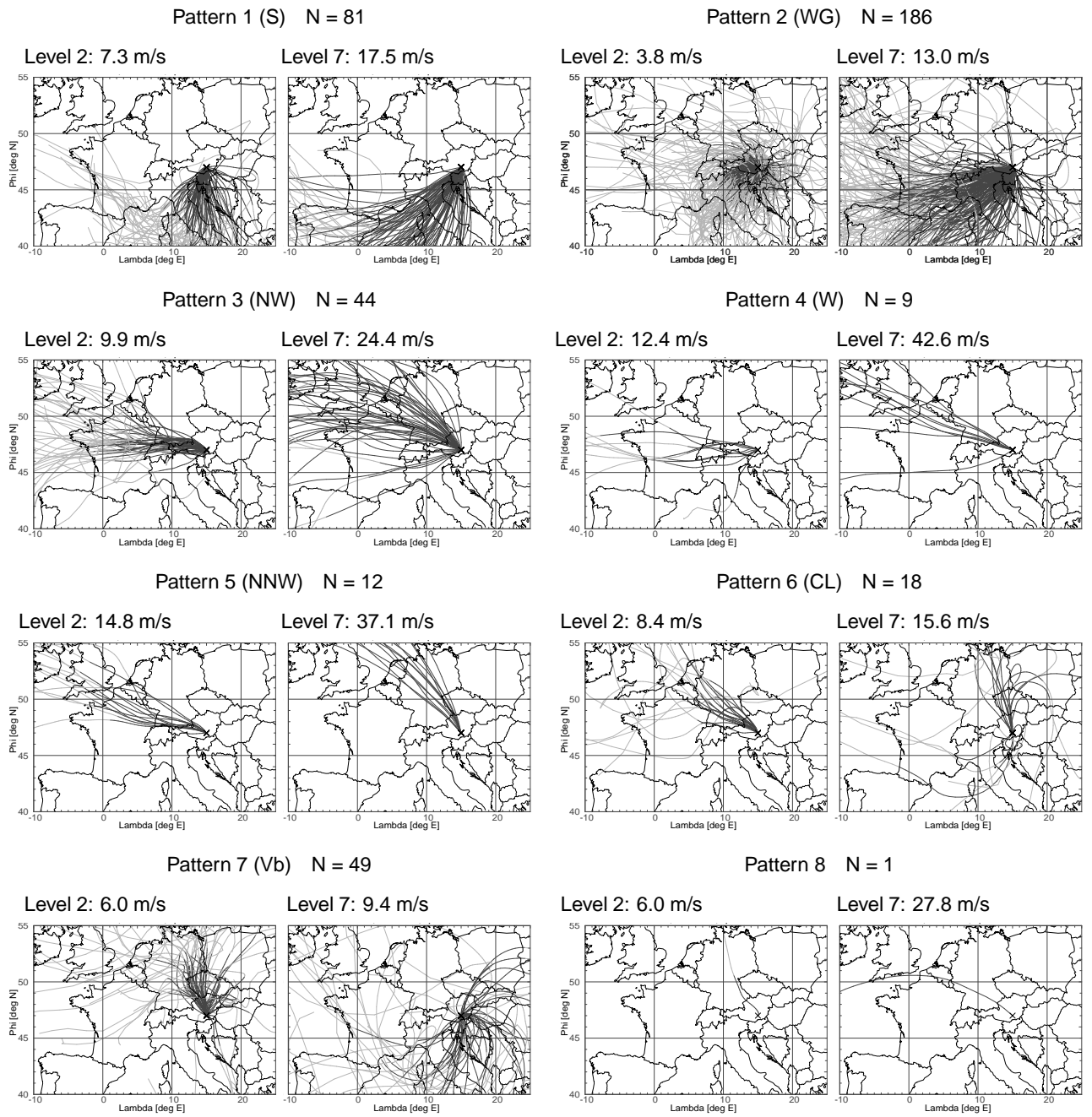
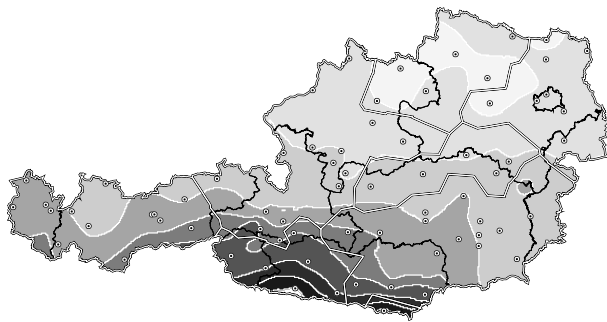
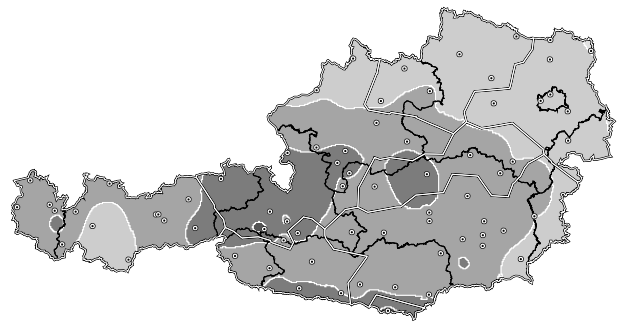


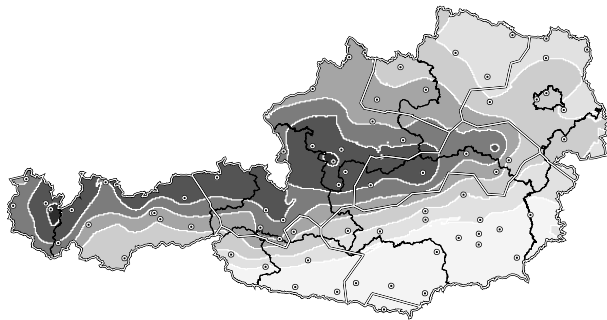
Figure 3: Back trajectories for the eight synoptic patterns found for heavy-precipitation days in Austria. Each pair of maps represents arrival at two different levels (left-hand frame: level 2 or 500 m agl, right-hand frame: level 7 or 500 hPa) and the south-eastern arrival point at 16:30 UTC. The number of cases (totally 400 in 15 years) as well as the mean wind velocity along the trajectories during the last 24 hours is given above the respective maps. The last 24 hours of every trajectory, which are used in the clustering, are printed in dark, whereas the remainder of every trajectory is printed in light grey.



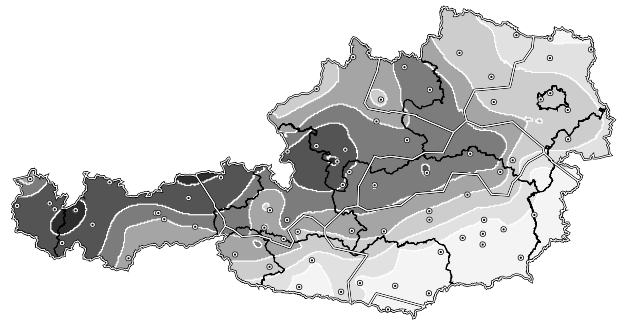
Pattern 1: Southerly "Stau"



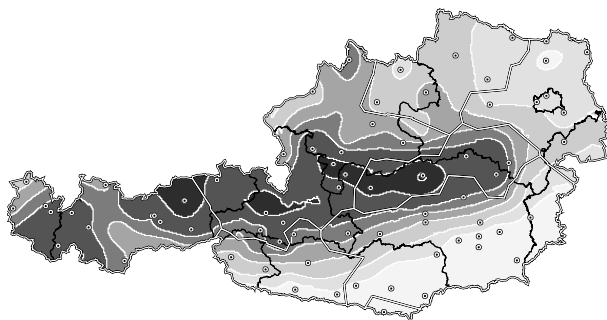
Pattern 2: Weak gradient



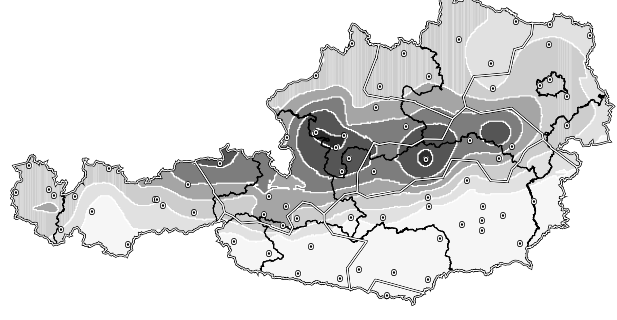
Pattern 3: Northwesterly flow



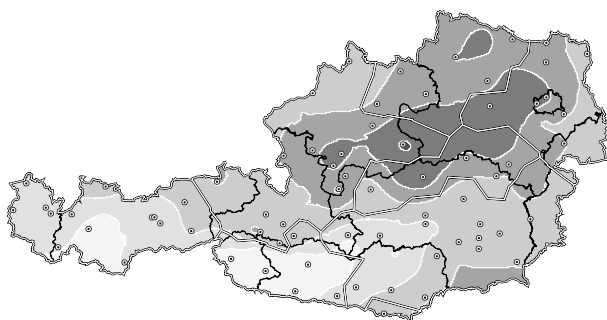
Pattern 4: Westerly "Stau"



Pattern 5: North-northwesterly flow



Pattern 6: Cut-off low to the east



Pattern 7: Vb-type situation

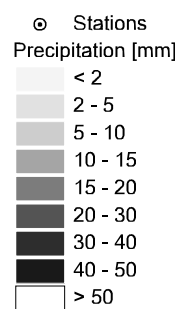


Figure 4: Median value of the daily precipitation for the seven synoptic patterns obtained by Kriging of the values at stations indicated by dots. The base are 400 days with heavy precipitation in at least one region of Austria. Double lines indicate the demarcation of the heavy-precipitation regions of Austria, and black lines the borders between the federal states of Austria.